Environmental Science & Technology

Article

pubs.acs.org/est

Enhanced Adsorption of Hydroxyl- and Amino-Substituted Aromatic Chemicals to Nitrogen-Doped Multiwall Carbon Nanotubes: A Combined Batch and Theoretical Calculation Study

Linzi Zuo,[†] Yong Guo,[‡] Xiao Li,[†] Heyun Fu,[†] Xiaolei Qu,[†] Shourong Zheng,[†] Cheng Gu,[†] Dongqiang Zhu,[*,†,§] and Pedro J. J. Alvarez[#]

[†]State Key Laboratory of Pollution Control and Resource Reuse and School of the Environment, Nanjing University, Nanjing, Jiangsu 210093, China

[‡]Key Laboratory of Integrated Regulation and Resource Development on Shallow Lakes, Ministry of Education, College of Environment, Hohai University, Nanjing, Jiangsu 210090, China

[§]School of Urban and Environmental Sciences, Peking University, Beijing 100871, China

[#]Department of Civil and Environmental Engineering, Rice University, Houston Texas 77005, United States

Supporting Information

ABSTRACT: A large effort is being made to develop nanosorbents with tunable surface chemistry for enhanced adsorption affinity and selectivity toward target organic contaminants. Heteroatom N-doped multiwall carbon nanotubes (N-MCNT) were synthesized by chemical vapor deposition of pyridine and were further investigated for the adsorptive removal of several aromatic chemicals varying in electronic donor and acceptor ability from aqueous solutions using a batch technique. Compared with commercial nondoped multiwall carbon nanotubes (MCNT), N-MCNT had similar specific surface area, morphology, and pore-size distribution but more hydrophilic surfaces and more surface defects due to the doping of graphitic and pyridinic N atoms. N-MCNT exhibited enhanced adsorption (2−10 folds) for the π-donor chemicals (2-naphthol and 1-naphthalmine) at pH ∼6 but similar adsorption for the weak π-donor chemical (naphthalene) and even lower adsorption (up to a 2-fold change) for the π-acceptor chemical (1,3-dinitrobenzene). The enhanced adsorption of 2-naphthol and 1-naphthalmine to N-MCNT was mainly attributed to the favored $\pi-\pi$ electron-donor−acceptor (EDA) interaction between the π-donor adsorbate molecule and the polarized N-heterocyclic aromatic ring (π-acceptor) on N-MCNT. The proposed adsorption enhancement mechanisms were further tested through the pH effects on adsorption and the density function theory (DFT) calculation. The results show for the first time that the adsorptive interaction of π-donor aromatic compounds with carbon nanomaterials can be facilitated by N-doping.

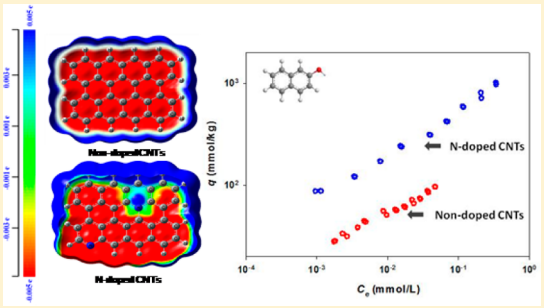

INTRODUCTION

Owing to their unique physical and chemical properties, carbon nanotubes have been considered as promising candidates for many nanoenabled environmental applications such as chemosensors in environmental monitoring, preconcentrators for organic analytes, and effective adsorbents for undesirable chemicals in water and wastewater treatment.[1−4] The relatively large specific surface area, combined with the very high surface hydrophobicity of carbon nanotubes, makes them superior adsorbents for hydrophobic organic contaminants in aqueous solutions.[3,4]

Numerous studies have been devoted to understanding the specific adsorptive interaction, particularly the structure−activity correlation, between organic chemicals and carbon nanotubes.[5−16] One important finding from these studies is that the sp^2-bonded graphitic sheets of carbon nanotubes are highly polarizable and are capable of inducing strong $\pi-\pi$ stacking and coupling with aromatic compounds.[5−11] Specific $\pi-\pi$ electron-donor−acceptor (EDA) interaction has also been proposed to account for the enhanced adsorption of π-electron-donor compounds (e.g., aromatics substituted with electron-donating groups such as amino and hydroxyl) and π-electron-acceptor compounds (e.g., nitroaromatics and tetracyclines substituted with electron-withdrawing groups such as nitro and ketone) to carbon nanomaterials relative to those compounds that are neither π donors nor π acceptors (e.g., benzene and chlorinated benzenes).[8,10−13,16] Resulting primarily from the polarization of edge and surface defects (i.e., due to functional substitution), carbonaceous materials including carbon nanotubes contain

Received: October 10, 2015
Revised: December 2, 2015
Accepted: December 15, 2015
Published: December 15, 2015

DOI: 10.1021/acs.est.5b04980
Environ. Sci. Technol. 2016, 50, 899−905

electron-rich sites and electron-depleted sites,[11,17−19] which can interact, respectively, with π-electron-acceptor compounds and π-electron-donor compounds via the π−π EDA mechanism. Additionally, electrostatic force and polar interactions (such as Lewis-acid−base interaction and H-bonding) can be important factors contributing to adsorption of charged or highly polar organic solutes to functionalized carbon nanotubes.[11,14] Consequently, a large effort is being made to optimize the specific adsorptive interaction of priority pollutants for enhanced affinity and selectivity through tuning the surface chemistry of carbon nanomaterials.[13,20,21]

Heteroatom doping is a useful approach to tailor the structural, electronic, and optical properties of carbon nanomaterials for developing new and improved nanotechnologies (such as supercapacitors and electrocatalyst).[22−24] However, few studies have been performed to systematically investigate the adsorption properties of environmentally relevant organic chemicals to heteroatom-doped carbon nanomaterials in aqueous solutions. Doping heteroatoms (e.g., N or B) into the graphitic lattice may significantly modify the surface chemistry of carbon nanotubes and in turn, affect their adsorption affinity for organic contaminants. For instance, protonated pyridinic N can not only introduce positive charge sites on the surface of carbon nanotubes but may also increase the π-electron acceptance ability of the associated aromatic rings due to its strong electron-withdrawing ability. It is reasonable to infer that the unique surface chemistry of heteroatom-doped carbon nanotubes can lead to different adsorption properties compared with those of nondoped carbon nanotubes.

The primary objective of this study was to use N-doped multiwall carbon nanotubes (N-MCNT) as a model nanosorbent with tunable surface chemistry for enhanced adsorption affinity and selectivity toward target organic contaminants. Batch adsorption isotherms of six adsorbates varying pronouncedly in electronic donating and accepting ability to N-MCNT were compared with those to commercial nondoped multiwall carbon nanotubes (MCNT). The effect of pH on adsorption to both carbon nanotubes was assessed to better illustrate the underlying mechanisms that govern adsorptive interaction; the pH can significantly affect the electronic properties and charge distribution of both adsorbate molecules and carbon nanotubes as their functional groups undergo the protonation−deprotonation transition. The proposed factors affecting adsorption to N-MCNT specifically were examined by the density function theory (DFT) calculation. Implication of the findings was further discussed.

EXPERIMENTAL SECTION

Adsorbates. The six test adsorbates are 2-naphthol (99%, Aldrich), 1-naphthylamine (98%, Sigma), naphthalene (99%, Sigma-Aldrich), 1,3-dinitrobenzene (97%, Sigma-Aldrich), *n*-octanol (99%, J&K Chemical), and triethanolamine (99.5%, Aladdin). Selected physicochemical properties of the adsorbates are listed in Table S1, and their molecular structures are shown in Figure S1.

Adsorbents. N-MCNT were synthesized by chemical vapor deposition of pyridine using Fe−Co as catalysts according to the literature method.[25] MCNT were purchased from Nanotech Port Co. (Shenzhen, Guangdong Province, China). On the basis of the information provided by the manufacturer, MCNT were also synthesized by a chemical vapor deposition method using cobalt, magnesium, or nickel as catalysts. MWNT contained carbon nanotubes with outer diameters ranging from 10 to 30 nm, and the length ranged from 5 to 15 μm, with <5% impurities (heavy metal catalysts and amorphous carbon). The N-MCNT and MCNT samples were treated by heating (350 °C for 30 min) followed by mixing with 70% (w/v) sodium hypochlorite aqueous solution to remove amorphous carbon and trace heavy metals using a previously developed method.[26]

Characterization of Adsorbents. Surface elemental compositions of the two carbon nanotubes were measured by X-ray photoelectron spectroscopy (XPS) (PerkinElmer PHI 550 ESCA/SAM, USA). N_2 adsorption and desorption isotherms were obtained on a Micrometrics ASAP 2020 (Micromeritics Instrument Co., Norcross, GA) apparatus at −196 °C (77 K) to measure specific surface area and pore-size distribution. To test the surface hydrophilicity of the two carbon nanotubes, we obtained sorption and desorption isotherms of water vapor on a DVS Intrinsic apparatus (Surface Measurement Systems Co., London, U.K.) at 25 °C (298 K). The two carbon nanotubes were also characterized by transmission electron microscopy (TEM), X-ray diffraction (XRD) analysis, and Raman spectra. The ζ potential of the two carbon nanotubes suspended in 0.001 mol/L NaCl solution equilibrated at different pH was measured using a ζ-potential analyzer (ZetaPALS; Brookhaven Instruments Corp., Holtsville, NY). The pK_a of nitrogen species in N-MCNT was determined by potentiometric titration using a microcomputer automatic potentiometric titrator (WDDY-2008, Datang, China).

Batch Adsorption. Adsorption experiments were conducted using a batch approach developed in our previous studies.[8,16] All adsorption isotherm experiments were run in duplicate. To initiate the experiments, we transferred about 20 mg carbon nanotubes to a 8 mL (for triethanolamine) or 40 mL (for other adsorbates) amber U.S. Environmental Protection Agency vial equipped with polytetrafluoroethylene-lined screw cap, followed by an electrolyte solution containing 0.02 mol/L NaCl. Afterward, the stock solution of the adsorbate (prepared in pure water for triethanolamine and in methanol for other solutes) was added to the vial, and the volume percentage of methanol, if used, was kept below 0.1% to minimize cosolvent effects. The initial concentrations were 0.0089−0.57 mmol/L for 2-naphthol, 0.044−0.52 mmol/L for 1-naphthylamine, 0.00085−0.19 mmol/L for naphthalene, 0.0016−0.12 mmol/L for 1,3-dinitrobenzene, 0.0078−0.093 mmol/L for *n*-octanol, and 0.033−0.34 mmol/L for triethanolamine. The vial was then filled with the electrolyte solution to leave minimal headspace, covered with aluminum foil, and tumbled at room temperature for 3 days to reach apparent adsorption equilibrium (no further uptake of solute), a conclusion based on the predetermined adsorption kinetics (see the Supporting Information).

After centrifugation at 2000 rpm for 15 min, the samples were left undisturbed for at least 30 min to allow the complete settling of the adsorbent. Concentration of *n*-octanol in the aliquot was analyzed by a Trace GC Ultra coupled to an ISQ mass spectrometer (Thermo Fisher Scientific), and triethanolamine was analyzed by ion chromatography (Dionex ICS-1000) consisting of an IonPac CS17 column (4 mm × 250 mm) under acidic conditions (pH 2.3) to ensure that the solute was in the protonated form. All other solutes were analyzed by high-performance liquid chromatography (HPLC) (Agilent 1200) with an ultraviolet detector using a 4.6 × 150 mm SB-C18

DOI: 10.1021/acs.est.5b04980
Environ. Sci. Technol. 2016, 50, 899−905

column (Agilent). Isocratic elution was performed under the following conditions: acetonitrile−water (60/40, v:v) with a wavelength of 230 nm for 2-naphthol; acetonitrile−water (50/50, v:v) with a wavelength of 254 nm for 1-naphthylamine; methanol−water (75/25, v:v) with a wavelength of 254 nm for naphthalene; methanol−water (60/40, v:v) with a wavelength of 238 nm for 1,3-dinitrobenzene. To take account for possible solute loss from processes other than adsorbent sorption (sorption to glassware and septum and volatilization), we obtained calibration curves separately from controls receiving the same treatment as the adsorption samples but no adsorbent. Calibration curves included at least 14 standards over the test concentration range. Based on the obtained calibration curves, we calculated the adsorbed mass of solute by subtracting mass in the aqueous phase from mass added. The equilibrium pH as measured at the end of the adsorption experiments was 6.0 ± 0.2. No peaks were detected in the HPLC spectra for potentially degraded or transformed products of the test adsorbates, as compared with freshly prepared control samples.

Another set of single-point batch adsorption experiments was conducted to test the pH dependency of adsorption to N-MCNT and MCNT for all adsorbates except *n*-octanol over pH 3.3−10.5 using the above-mentioned method. The initial concentration was 0.26 mmol/L for 2-naphthol, 0.50 mmol/L for 1-naphthylamine, 0.007 mmol/L for naphthalene, 0.03 mmol/L for 1,3-dinitrobenzene, and 0.23 mmol/L for triethanolamine. The experiments were run in triplicate.

DFT Theoretical Calculation. The interaction energies of 2-naphthol (π-donor) and 1,3-dinitrobenzne (π-acceptor) with a model graphene nanoribbon ($C_{36}H_{16}$) and its N-doped counterpart were calculated using the Gaussian 09(5)[27] program at the M062*x*/6-31g(d,p)(4) level.[28] The number of doping N atoms was set to two (corresponding to 6.19% nitrogen on a weight basis), and the combinations were two graphitic nitrogens, two pyridinic nitrogens, and one graphitic nitrogen and one pyridinic nitrogen. The pyridinic nitrogen(s) was either protonated or deprotonated.

RESULTS AND DISCUSSION

Characterization of Adsorbents. The information on surface elemental compositions and surface areas of the two carbon nanotubes is summarized in Table 1. Both carbon nanotubes were predominated by graphitized C (>86%) on the surfaces and contained relatively low surface oxygen contents (7.30% for N-MCNT and 8.34% for MCNT); N-MCNT contained 6.02% surface nitrogen content. On the basis of the method in the literature,[29] the deconvolution of the nitrogen peak in the XPS spectrum revealed the following nitrogen species distribution on N-MCNT: 44.42% graphitic N, 44.98% pyridinic N, and 10.60% nitrogen oxides. The two carbon nanotubes had very close specific surface areas (118.0 m^2/g for N-MCNT and 130.8 m^2/g for MCNT), similar nanotubular morphologies (as reflected by the TEM images; see Figure S2), and similar pore-size distribution profiles (Figure S3). When compared with MCNT, N-MCNT contained less ordered, lower-sized graphitic sheets, which is indicative of more edge sites and surface defects. This was supported by comparing the XRD patterns and Raman spectra between the two carbon nanotubes (see more details in Figures S4−S5).

Table 1. Surface Elemental Compositions (Dry-Weight-Based) and Surface Areas of Nitrogen-Doped Multiwall Carbon Nanotubes (N-MCNT) and Nondoped Multiwall Carbon Nanotubes (MCNT)

	surface elemental composition[a]			
adsorbent	C%	O%	N%	surface area(m^2/g)[b]
N-MCNT	86.66	7.30	6.03	118.0
MCNT	90.49	8.34	BDL[c]	130.8

[a]Determined by X-ray photoelectron spectroscopy. [b]Determined by N_2 adsorption using the Brunauer−Emmett−Teller method. [c]Below detectable level.

As shown from the ζ potential−pH relationship (Figure S6), the surface of N-MCNT was consistently less negatively charged than the surface of MCNT within the pH range of 2.0 to 11.8. Moreover, the surface of N-MCNT became positively charged at very low pH (around 2). The pK_a of the pyridinic nitrogen groups on N-MCNT as measured from the acid−base titration was approximately 5.6, consistent with the values (between 5 and 6) reported in the literature.[30] These pyridinic nitrogen groups can thus act as weak bases and become protonated and positively charged at low pH, neutralizing the negative charges from the deprotonated surface oxygen groups (mainly carboxyls). Figure 1 presents the adsorption−desorption isotherms of water vapor to MCNT and N-MCNT. Given the same vapor pressure, N-MCNT adsorbed more than twice the amount of water compared with that absorbed by MCNT. It was shown in previous studies that the adsorption affinity of water vapor positively correlated with the surface hydrophilicity of adsorbents.[31,32] The observations made herein indicate that the surface of N-MCNT was more hydrophilic than the surface of MCNT, attributing to the highly-polar- or highly-ionizable-surface nitrogen groups. The higher surface hydrophilicity of N-MCNT would provide an extra benefit to enhance mass transfer and hydrodynamics in a nanotube-packed column or a nanotube-incorporated membrane that has shown a great potential in water and wastewater treatment.[3,33−35]

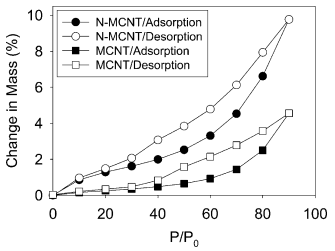

Figure 1. Water-vapor adsorption and desorption isotherms on N-doped multiwall carbon nanotubes (N-MCNT) and nondoped multiwall carbon nanotubes (MCNT).

Adsorption Isotherms. Figure 2 compares adsorption isotherms, plotted as adsorbed concentration (q, mmol/kg) versus aqueous-phase concentration (C_e, mmol/L) at adsorption equilibrium, to N-MCNT and MCNT for different adsorbates. The Freundlich sorption model fits the isotherm data reasonably (R^2 > 0.83); the model fitting results, along with the ranges of adsorption-distribution coefficients (K_d, L/kg) are shown in Table S2.

Depending on the test adsorbate molecules, N-MCNT and MCNT exhibited different trends of relative adsorption affinities. For 2-naphthol and 1-naphthalmine, adsorption to N-MCNT was much higher (2−10 folds) than adsorption to MCNT. However, for the rest of the test adsorbates, adsorption

DOI: 10.1021/acs.est.5b04980
Environ. Sci. Technol. 2016, 50, 899−905

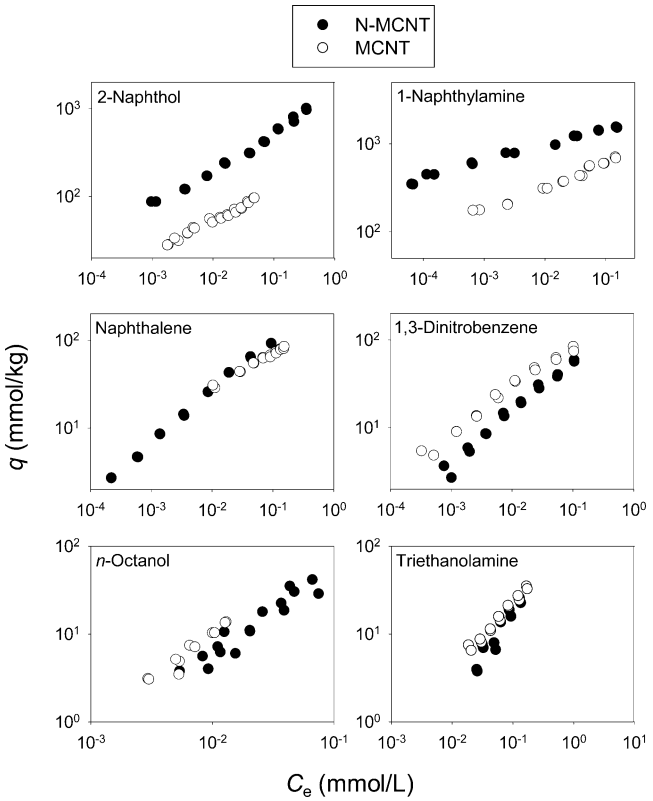

Figure 2. Adsorption isotherms plotted as adsorbed concentration (q, mmol/kg) vs aqueous-phase concentration (C_e, mmol/L) at adsorption equilibrium for different compounds on N-doped multiwall carbon nanotubes (N-MCNT) and nondoped multiwall carbon nanotubes (MCNT).

to N-MCNT was close to or even lower than adsorption to MCNT. As strong electron-donating groups,[36] the −OH of 2-naphthol and the $-NH_2$ of 1-naphthylamine make the substituted naphthalene rings rich in π-electron, and thus, allowing these two chemicals to interact strongly with the polarized electron-depleted region on the graphitic surfaces of carbon nanotubes via the $\pi-\pi$ EDA mechanism.[12] Compared with the nondoped aromatic rings on MCNT, the π-electron accepting ability of the N-heterocyclic aromatic ring on N-MCNT is increased due to the high electron negativity of N atom, resulting in enhanced $\pi-\pi$ EDA interaction with the π-electron-donor chemicals (2-naphthol and 1-naphthylamine). This helps to explain the significant upward displacement of the adsorption isotherms of these two chemicals to N-MCNT relative to MCNT. It is understandable that for naphthalene, a very weak π-electron donor, the adsorption isotherms to MCNT and N-MCNT nearly overlapped. In contrast to 2-naphthol and 1-naphthalmine, adsorption of 1,3-dinitronbzene was obviously lower to N-MCNT than to MCNT. Due to the very strong electron-withdrawing ability of the $-NO_2$ group, the benzene ring of 1,3-dinitrobenzene is electron-depleted and hence can be considered as an effective π-electron acceptor. Stemming from the electron-withdrawing effect of the N atoms, the overall π-electron-donor ability of the graphitic surface on N-MCNT should be lower than the graphitic surface on MCNT; as a result, the $\pi-\pi$ EDA interaction between 1,3-dinitrobenzene and N-MCNT was impeded to some extent.

Both the graphitic N and the pyridinic N are able to withdraw electrons from the neighboring carbon atoms on the graphitic surface. Owing to the higher degree of electronic conjugation of carbon−nitrogen bonds, the graphitic N-heterocyclic aromatic ring has stronger π-electron accepting ability than the pyridinic N-heterocyclic aromatic ring. However, the electron-accepting ability of pyridinic N-heterocyclic aromatic ring is expected to be pH-dependent. Once the N atom is protonated, the positively charged N-heterocyclic aromatic ring acts as a stronger π-acceptor than the neutral nonprotonated counterpart. At the test pH of 6.0, approximately 28.5% of the pyridinic N atoms (equivalent to 1.2 mol-N/kg-adsorbent) were protonated, further facilitating the $\pi-\pi$ EDA interaction with 2-naphthol and 1-naphthylamine.

One may argue that H-bonding between the adsorbate −OH or $-NH_2$ group and the nitrogen groups on N-MCNT could be the primary adsorption-enhancement mechanism. However, this hypothesis can be ruled out by the experimental observation and the literature studies. The adsorption isotherms of *n*-octanol (a model hydrogen bonder) were very close between MCNT and N-MCNT (see Figure 2), suggesting that H-bonding played a minimal role or equal role in adsorption to the two carbon nanotubes. Previous studies based on DFT and molecular mechanics calculations also proposed that the H-bonding between phenol and the O-containing groups on activated carbon was negligible due to the competitive and much stronger interactions of water molecules.[37] Another plausible mechanism for the enhanced adsorption of 2-naphthol and 1-naphthylamine to N-MCNT could be Lewis-acid−base interaction, where 2-naphthol or the protonated nitrogen group on N-MCNT serves as the Lewis acid and 1-naphthylamine or the nonprotonated nitrogen group serves as the Lewis base. This mechanism has been explored previously to explain the extraordinarily strong adsorption of amino-substituted aromatic chemicals to carbon nanomaterials containing fairly high amounts of surface oxygen groups.[12,38] However, Lewis-acid−base interaction was not likely the primary cause for the enhanced adsorption of 1-naphthylamine to N-MCNT, as evidenced by the fact that N-MCNT and MCNT exhibited nearly overlapping triethanolamine adsorption (Figure 2). Because the two lone-pair electrons on the N atom are not involved in the π-electron system, triethanolamine is a much stronger Lewis base than 1-naphthylamine (also reflected by the higher pK_a of triethanolamine; see Table S1).

Effects of pH on Adsorption. Figure 3 displays the relationship of K_d (L/kg) versus pH for single-point adsorption of different adsorbates to N-MCNT and MCNT. For 2-naphthol, the adsorption to N-MCNT increased with pH, reaching the maximum level at pH close to its pK_a value but then decreased when the pH was further increased; however, the adsorption to MCNT increased slightly but consistently with pH, even when the pH was above the pK_a value. At pH higher than the pK_a value (9.51), 2-naphthol is dominated by the negatively charged form, leading to combined effects on adsorption. First, the adsorption of 2-naphthol would be hindered due to a combination of decreased solute hydrophobicity and the repulsive electrostatic interaction with the negatively charged surface O-containing groups. Second, when −OH is deprotonated to $-O^-$ at high pH, the electron-donating ability would be further improved, leading to enhanced $\pi-\pi$ EDA interaction. The relative importance of these two factors depends on the distribution and abundance of the active sites (surface O-containing and heterocyclic N atoms) involved in adsorption. Nonetheless, within the whole

DOI: 10.1021/acs.est.5b04980
Environ. Sci. Technol. 2016, 50, 899−905

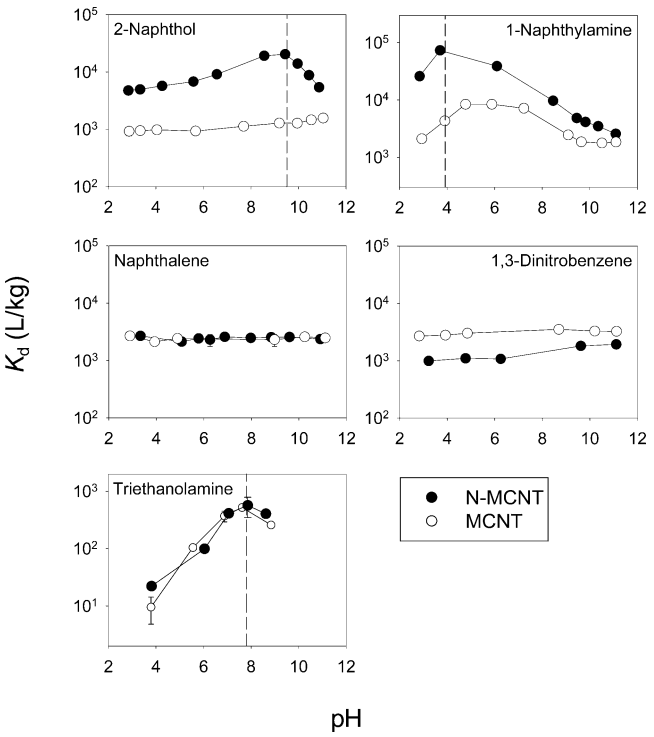

Figure 3. Single-point adsorption on N-doped multiwall carbon nanotubes (N-MCNT) and non-doped multiwall carbon nanotubes (MCNT) plotted as solid-to-solution distribution coefficient (K_d, L/kg) vs pH for different compounds. Error bars, in most cases smaller than the symbols, represent standard deviations calculated from triplicate samples. The vertical lines represent values of acid dissociation constants (pK_a) of compounds (if applicable). The solid trend lines are for clarity only.

pH range examined, adsorption of 2-naphthol to N-MCNT was significantly higher than that to MCNT, indicating that $\pi-\pi$ EDA interaction with the N-heterocyclic aromatic ring was the predominant adsorption-enhancement mechanism.

For both MCNT and N-MCNT, 1-naphthylamine and triethanolamine showed bell-shaped pH-dependency curves, with the peak at pH near the adsorbate pK_a. At pH lower than the respective pK_a values, 1-naphthylamine and triethanolamine are dominated by the protonated forms, and the Lewis-acid–base interaction with the acidic surface groups on the carbon nanotubes would be impeded. However, the Lewis-acid–base interaction would also become weaker with increasing pH because the acidic surface groups on the carbon nanotubes are mostly deprotonated. The fact that the maximum triethanolamine adsorption occurred at pH close to the pK_a value (7.8) also implies an insignificant role of electrostatic attraction played in adsorption. Otherwise, the maximum triethanolamine adsorption would have occurred at lower pH around 6, wherein the two carbon nanotubes had the lowest negative surface charge (see Figure S6); meanwhile, triethanolamine was predominated by the positively charged form. Within the test pH range, adsorption of 1-naphthylamine to N-MCNT was consistently higher than that to MCNT, whereas the pH-dependency curves of triethanolamine were nearly overlapping between the two adsorbents. The results confirm that the enhanced adsorption of 1-naphthylamine to N-MCNT was mainly caused by $\pi-\pi$ EDA interaction rather than Lewis-acid–base interaction with the N-heterocyclic aromatic ring.

The pH effect on adsorption of naphthalene to MCNT and N-MCNT was minimal. It appeared that the protonation–deprotonation transition of the surface functional groups on the carbon nanotubes had negligible effect on the adsorptive affinity. Naphthalene is nonpolar and possesses very weak electron-donor ability, and therefore, its adsorption would be mainly controlled by the nonspecific $\pi-\pi$ coupling (mainly dispersion interaction) with the graphitic surfaces on the carbon nanotubes.[10] It is interesting to note that for 1,3-dinitrobenzene, the adsorption to MCNT and N-MCNT slightly increased with increasing pH, with more significant effects observed for N-MCNT. Increasing pH facilitated deprotonation of the acidic functional groups (−COOH, −OH, and protonated pyridinic N) of the carbon nanotubes and promoted the π-electron-donor ability of the associated graphitic surfaces, therefore facilitating the $\pi-\pi$ EDA interaction of 1,3-dinitrobenzene (π-acceptor). The stronger pH dependency in adsorption to N-MCNT compared with MCNT can be attributed to the effect of extra pyridinic nitrogen groups on N-MCNT.

DFT Theoretical Calculation. Figure 4 displays the electron distributions of the model single-layered graphene

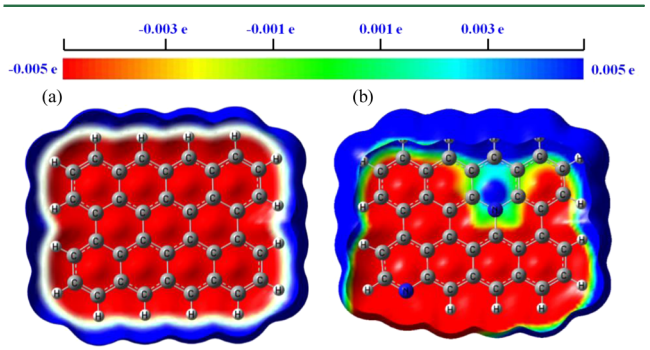

Figure 4. Electron-density distributions of single-layered graphene nanoribbon (N-GN) and N-doped graphene nanoribbon (GN) containing two nitrogen atoms. (a) GN; (b) N-GN and (NP–NG). N_P represents nonprotonated pyridinic nitrogen, and N_G represents graphitic nitrogen.

nanoribbon (GN) and N-doped graphene nanoribbon (N-GN) containing two nitrogen atoms. Because of the higher electronegativity of the carbon atom as compared with the hydrogen atom, the electrons are highly polarized along GN, with the higher electron density in the center (colored red) and the lower electron density at the edge (colored blue), which serve as π-electron-donor and π-electron-acceptor sites, respectively. After the replacement of two carbon atoms by two nitrogen atoms, the electron density in the region (colored light blue) surrounding the nitrogen atom is substantially lowered due to the very high electronegativity of the nitrogen atom, resulting in higher degree of electron polarization. The gas-phase interaction energies (ΔE, kJ/mol) between 2-naphthol (model π-donor) and 1,3-dinitrobenzene (model π-acceptor) and GN and N-GN were further calculated based on the DFT theory (results presented in Table 2). For 2-naphthol, the ΔE value is increased by 7.1–19.2 kJ/mol after N-doping, and the highest increment is shown for the nanoribbon containing two graphitic nitrogen atoms (N_G–N_G). This is because compared with the pyridinic nitrogen, the graphitic nitrogen is more involved in electronic conjugation with neighboring carbon atoms; in addition, the electron-acceptor

DOI: 10.1021/acs.est.5b04980
Environ. Sci. Technol. 2016, 50, 899–905

Table 2. Gas-Phase Interaction Energies (ΔE, kJ/mol) between Selected Adsorbates and Model Graphene Nanoribbon (GN) and N-Doped Graphene Nanoribbon (N-GN) Containing Two Nitrogen Atoms from DFT Calculation

	ΔE (kJ/mol)					
		N-GN				
adsorbate	GN	N_P-N_G[a]	$N_P^+-N_G$[b]	N_P-N_P[c]	$N_P^+-N_P^+$[d]	N_G-N_G[e]
2-naphthol	−55.2	−64.0	−67.3	−62.3	−66.9	−74.4
1,3-dinitrobenzene	−68.8	−69.8	−69.0	−68.4	−62.6	−69.9

[a]One pyridinic nitrogen and one graphitic nitrogen. [b]One protonated pyridinic nitrogen and one graphitic nitrogen. [c]Two pyridinic nitrogens. [d]Two protonated pyridinic nitrogens. [e]Two graphitic nitrogens.

sites induced by the graphitic nitrogen are located close to the center rather than at the edge of the nanoribbon, thus facilitating the face-to-face $\pi-\pi$ EDA complexation of the 2-naphthol molecule. In the case of pyridinic N-doping, the ΔE value is increased by 3−5 kJ/mol when the nitrogen atom(s) is protonated. For 1,3-dinitrobenzene, the ΔE value keeps nearly constant between GN and N-GN with the exception of N-GN containing two protonated pyridinic nitrogen atoms ($N_P^+-N_P^+$), for which the ΔE value is decreased by 6.2 kJ/mol. Thus, the DFT calculation results are generally in good agreement with the experimental adsorption data.

Implication. The advantage of tunable surface chemistry on the nanoscale endows carbon nanomaterials with a wide variety of emerging environmental applications, such as effective and selective adsorbents for organic contaminants. The most striking finding of this study is that heteroatom N-doped carbon nanotubes exhibit much higher adsorption affinity and selectivity for π-donor (including but not limited to hydroxyl- and amino-substituted) aromatic compounds than nondoped carbon nanotubes. Compared with nondoped carbon nanotubes, N-doped carbon nanotubes have much more hydrophilic surfaces, which would substantially mitigate the hydrodynamic sheer force and lower the energy cost when the nanomaterials are used as adsorbents for column cleanup and separation of target organic chemicals. Likewise, due to the more ionic and polar nature, N-doped carbon nanotubes are expected to be more compatible with hydrophilic polymeric materials (such as poly(ether sulfone)) for designing multifunctional composite membranes in water and wastewater treatment. More research on the environmental application of N-doped carbon nanotubes as unique adsorbents is warranted.

■ ASSOCIATED CONTENT

Supporting Information

The Supporting Information is available free of charge on the ACS Publications website at DOI: 10.1021/acs.est.5b04980.

Properties of the adsorbates (Table S1 and Figure S1), adsorption-model fitting parameters (Table S2), characterization of the adsorbents (Figures S2−S6), and adsorption kinetics (Figure S7). (PDF)

■ AUTHOR INFORMATION

Corresponding Author

*Phone: +86 (010) 62766405; e-mail: zhud@pku.edu.cn.

Notes

The authors declare no competing financial interest.

■ ACKNOWLEDGMENTS

We thank the High-Performance Computing Center of Nanjing University for the computational study. This work was supported by the National Natural Science Foundation of China (grants 21237002, 21225729, and 21428701).

■ REFERENCES

(1) Baughman, R. H.; Zakhidov, A. A.; de Heer, W. A. Carbon nanotubes − The route toward applications. *Science* **2002**, *297* (5582), 787−792.

(2) Tasis, D.; Tagmatarchis, N.; Bianco, A.; Prato, M. Chemistry of carbon nanotubes. *Chem. Rev.* **2006**, *106* (3), 1105−1136.

(3) Mauter, M. S.; Elimelech, M. Environmental applications of carbon-based nanomaterials. *Environ. Sci. Technol.* **2008**, *42* (16), 5843−5859.

(4) Ren, X.; Chen, C.; Nagatsu, M.; Wang, X. Carbon nanotubes as adsorbents in environmental pollution management: A review. *Chem. Eng. J.* **2011**, *170* (2−3), 395−410.

(5) Long, R.; Yang, R. Carbon nanotubes as superior sorbent for dioxin removal. *J. Am. Chem. Soc.* **2001**, *123* (9), 2058−2059.

(6) Fagan, S. B.; Souza Fiho, A. G.; Lima, J. O. G.; Filho, J. M.; Ferreira, O. P.; Mazali, I. O.; Alves, O. L.; Dresselhaus, M. S. 1,2-Dichlorobenzene interacting with carbon nanotubes. *Nano Lett.* **2004**, *4* (7), 1285−1288.

(7) Gotovac, S.; Honda, H.; Hattori, Y.; Takahashi, K.; Kanoh, H.; Kaneko, K. Effect of nanoscale curvature of single-walled carbon nanotubes on adsorption of polycyclic aromatic hydrocarbons. *Nano Lett.* **2007**, *7* (3), 583−587.

(8) Chen, W.; Duan, L.; Zhu, D. Adsorption of polar and nonpolar organic chemicals to carbon nanotubes. *Environ. Sci. Technol.* **2007**, *41* (24), 8295−8300.

(9) Kar, T.; Bettinger, H. F.; Scheiner, S.; Roy, A. K. Noncovalent π-π stacking and CH-π interactions of aromatics on the surface of single-wall carbon nanotubes: An MP2 study. *J. Phys. Chem. C* **2008**, *112* (50), 20070−20075.

(10) Chen, J.; Chen, W.; Zhu, D. Adsorption of nonionic aromatic compounds to single-walled carbon nanotubes: Effects of aqueous solution chemistry. *Environ. Sci. Technol.* **2008**, *42* (19), 7225−7230.

(11) Pan, B.; Xing, B. Adsorption mechanisms of organic chemicals on carbon nanotubes. *Environ. Sci. Technol.* **2008**, *42* (24), 9005−9013.

(12) Chen, W.; Duan, L.; Wang, L. L.; Zhu, D. Adsorption of hydroxyl- and amino-substituted aromatics to carbon nanotubes. *Environ. Sci. Technol.* **2008**, *42* (18), 6862−6868.

(13) Lu, C.; Su, F.; Hu, S. Surface modification of carbon nanotubes for enhancing BTEX adsorption from aqueous solutions. *Appl. Surf. Sci.* **2008**, *254* (24), 7035−7041.

(14) Yang, K.; Wu, W.; Jing, Q.; Zhu, L. Aqueous adsorption of aniline, phenol and their substitutes by multi-walled carbon nanotubes. *Environ. Sci. Technol.* **2008**, *42* (21), 7931−7936.

(15) Cho, H. H.; Smith, B. A.; Wnuk, J. D.; Fairbrother, D. H.; Ball, W. P. Influence of surface oxides on the adsorption of naphthalene onto multiwalled carbon nanotubes. *Environ. Sci. Technol.* **2008**, *42* (8), 2899−2905.

(16) Ji, L. L.; Chen, W.; Duan, L.; Zhu, D. Mechanisms for strong adsorption of tetracycline to carbon nanotubes: A comparative study using activated carbon and graphite as adsorbents. *Environ. Sci. Technol.* **2009**, *43* (7), 2322−2327.

DOI: 10.1021/acs.est.5b04980
Environ. Sci. Technol. 2016, 50, 899−905

(17) McDermott, M. T.; McCreery, R. L. Scanning tunneling microscopy of ordered graphite and glassy carbon surfaces: Electronic control of quinone adsorption. *Langmuir* **1994**, *10* (11), 4307−4314.
(18) Moreno-Castilla, C. Adsorption of organic molecules from aqueous solutions on carbon materials. *Carbon* **2004**, *42* (1), 83−94.
(19) Zhu, D.; Pignatello, J. J. Characterization of aromatic compound sorptive interactions with black carbon (charcoal) assisted by graphite as a model. *Environ. Sci. Technol.* **2005**, *39* (7), 2033−2041.
(20) Liao, Q.; Sun, J.; Gao, L. Adsorption of chlorophenols by multi-walled carbon nanotubes treated with HNO_3 and NH_3. *Carbon* **2008**, *46* (3), 553−555.
(21) Norzilah, A. H.; Fakhru'l-Razi, A.; Choong, T. S. Y.; Chuah, A. L. Surface modification effects on CNTs adsorption of methylene blue and phenol. *J. Nanomater.* **2011**, *2011*, 1−18.
(22) Gong, K.; Du, F.; Xia, Z.; Durstock, M.; Dai, L. Nitrogen-doped carbon nanotube arrays with high electrocatalytic activity for oxygen reduction. *Science* **2009**, *323* (5915), 760−764.
(23) Jeong, H. M.; Lee, J. W.; Shin, W. H.; Choi, Y. J.; Shin, H. J.; Kang, J. K.; Choi, J. W. Nitrogen-doped graphene for high-performance ultracapacitors and the importance of nitrogen-doped sites at basal planes. *Nano Lett.* **2011**, *11* (6), 2472−2477.
(24) Wang, X.; Sun, G.; Routh, P.; Kim, D. H.; Huang, W.; Chen, P. Heteroatom-doped graphene materials: Syntheses, properties and applications. *Chem. Soc. Rev.* **2014**, *43* (20), 7067−7098.
(25) Chen, H.; Yang, Y.; Hu, Z.; Huo, K.; Ma, Y.; Chen, Y.; Wang, X.; Lu, Y. Synergism of C_5N six-membered ring and vapor-liquid-solid growth of CN_x nanotubes with pyridine precursor. *J. Phys. Chem. B* **2006**, *110* (33), 16422−16427.
(26) Lu, C. Y.; Chiu, H. S. Adsorption of zinc(II) from water with purified carbon nanotubes. *Chem. Eng. Sci.* **2006**, *61* (4), 1138−1145.
(27) Frisch, M.; Trucks, G.; Schlegel, H.; Scuseria, G.; Robb, M.; Cheeseman, J.; et al. *Gaussian 09* (Revision A.02); Gaussian, Inc.: Wallingford CT, 2009.
(28) Zhao, Y.; Truhlar, D. G. The M06 suite of density functionals for main group thermochemistry, thermochemical kinetics, non-covalent interactions, excited states, and transition elements: Two new functionals and systematic testing of four M06-class functionals and 12 other functionals. *Theor. Chem. Acc.* **2008**, *120* (1−3), 215−241.
(29) Liu, H.; Zhang, Y.; Li, R.; Sun, X.; Désilets, S.; Abou-Rachid, H.; Jaidann, M.; Lussier, L. Structural and morphological control of aligned nitrogen-doped carbon nanotubes. *Carbon* **2010**, *48* (5), 1498−1507.
(30) Bitter, J. H.; van Dommele, S.; de Jong, K. P. On the virtue of acid-base titrations for the determination of basic sites in nitrogen doped carbon nanotubes. *Catal. Today* **2010**, *150* (1−2), 61−66.
(31) Karanfil, T.; Dastgheib, S. A. Trichloroethylene adsorption by fibrous and granular activated carbons: Aqueous phase, gas phase, and water vapor adsorption studies. *Environ. Sci. Technol.* **2004**, *38* (22), 5834−5841.
(32) Toth, A.; Voitko, K. V.; Bakalinska, O.; Prykhod'ko, G. P.; Bertoti, I.; Martinez-Alonso, A.; Tascon, J. M. D.; Gun'ko, V. M.; Laszlo, K. Morphology and adsorption properties of chemically modified MWCNT probed by nitrogen, *n*-propane and water vapor. *Carbon* **2012**, *50* (2), 577−585.
(33) Wang, X.; Chen, X.; Yoon, K.; Fang, D.; Hsiao, B. S.; Chu, B. High flux filtration medium based on nanofibrous substrate with hydrophilic nanocomposite coating. *Environ. Sci. Technol.* **2005**, *39* (19), 7684−7691.
(34) Celik, E.; Park, H.; Choi, H.; Choi, H. Carbon nanotube blended polyethersulfone membranes for fouling control in water treatment. *Water Res.* **2011**, *45* (1), 274−282.
(35) Dichiara, A. B.; Harlander, S. F.; Rogers, R. E. Fixed bed adsorption of diquat dibromide from aqueous solution using carbon nanotubes. *RSC Adv.* **2015**, *5* (76), 61508−61512.
(36) Carey, F. A. *Organic Chemistry*, 6th ed.; McGraw-Hill: New York, 2006.
(37) Efremenko, I.; Sheintuch, M. Predicting solute adsorption on activated carbon: Phenol. *Langmuir* **2006**, *22* (8), 3614−3621.
(38) Wang, F.; Haftka, J. J. H.; Sinnige, T. L.; Hermens, J. L. M.; Chen, W. Adsorption of polar, nonpolar, and substituted aromatics to colloidal graphene oxide nanoparticles. *Environ. Pollut.* **2014**, *186*, 226−233.

DOI: 10.1021/acs.est.5b04980
Environ. Sci. Technol. 2016, 50, 899−905